# Computational Fluid Dynamics Investigation of Thermal Performance in Helical Tube Radiators Using Ethanol Coolant under Variable Outlet

K. Kayastha[1*], P. A. Anadani[1], R. Parikh[1], R. Kokate[1], I. U. Rasoolbhai[2]

[1]Department of Mechanical Engineering, Parul University, Waghodia Road, Limda, Vadodara, India.
[2]Department of Civil Engineering, Parul University, Waghodia Road, Limda, Vadodara, India.

***ABSTRACT:*** Efficient thermal management is essential for maintaining the performance and reliability of automotive systems. While water–glycol mixtures are commonly used as coolants, alternative fluids such as ethanol require systematic evaluation under varying operating conditions. This study aims to investigate the effect of outlet pressure on the thermal–hydraulic performance of a helical tube radiator using ethanol as the working fluid. A three-dimensional CFD model was developed in ANSYS CFX 2021 R1 under steady-state, incompressible, and transition flow conditions. The simulations were performed at a constant mass flow rate of 2.3kg/s and inlet temperature of 371.75K, with outlet pressure varied from 0.25 to 2.5bar. The governing equations of continuity, momentum, and energy were solved using a finite volume approach with second-order discretization. Model validation was conducted using Dittus–Boelter and Darcy–Weisbach correlations, showing deviations within 5–6%. The results show that the maximum temperature drop of 12.58K occurs at 2.0bar, while the minimum of 9.63K occurs at 0.5bar, with only ~1.4% improvement over baseline. The pressure drop remains nearly constant (~8.93bar). It is concluded that ethanol reduces pumping resistance but does not outperform water-based coolants due to its lower thermal properties.

***KEYWORDS:*** Automotive radiator; CFD analysis; Ethanol coolant; Helical tubes; Heat transfer; Thermal performance; ANSYS CFX

[Received Dec. 25, 2025; Revised Feb. 24, 2026; Accepted Mar. 24, 2026] Print ISSN: 0189-9546 | Online ISSN: 2437-2110

## I. INTRODUCTION

Modern automotive engines produce considerable thermal energy during their operation, with roughly 30% of the total energy being released via the cooling system (He, 2023). Efficient thermal management is crucial for preserving engine efficiency, mitigating thermal fatigue, and guaranteeing vehicle reliability and extended lifespan. The automotive radiator serves as a vital element within this thermal management system, facilitating the transfer of engine heat to the ambient air through intricate fluid dynamics and convective heat transfer processes (Larkin, 2018).

Modern automotive engineering necessitates the development of more compact cooling systems that provide superior thermal performance in limited space. This requires a thorough examination of coolant flow, temperature distribution, and pressure changes in radiator tubes. Traditional design methods often depend on empirical correlations and experimental prototypes, which can be both costly and time-consuming. Consequently, computational fluid dynamics (CFD) has become a crucial tool for predicting thermal performance and refining radiator design before physical prototypes are built (Jouhara et al., 2021).

Recent progress in thermal fluid analysis has led to the exploration of alternative cooling fluids, moving beyond the traditional use of water-glycol mixtures. Ethanol has been considered as an alternative coolant primarily due to its lower viscosity and potential for reduced pumping power; however, its thermal conductivity and specific heat capacity are significantly lower than those of conventional water-based coolants, necessitating a critical evaluation of its overall heat transfer performance. This makes them a good choice for future cooling systems (Ebaid et al., 2017). However, a thorough evaluation of how well ethanol coolants work, considering different tube designs and operational conditions, is still missing in current research.

This investigation explores the thermal characteristics of helical tube radiators, utilizing ethanol as the coolant medium. The principal aims are threefold: first, to develop a validated computational fluid dynamics (CFD) methodology for radiator assessment, utilizing commercially available software; second, to assess the impact of outlet pressure fluctuations on thermal performance; and third, to determine the most favorable operational parameters for enhanced heat dissipation. The helical tube configuration was selected due to its capacity to enhance fluid mixing and heat transfer, offering advantages over straight tube designs, while also maintaining structural integrity (Webb, 2018).

Three-dimensional CFD simulations of tube-in-tube heat exchangers were performed using STAR-CD

*Corresponding author: *krunal.kayastha@paruluniversity.ac.in* ***doi:*** http://doi.org/10.63746/njtd.v23i1.4300

software, and experimental validation was integrated to establish foundational procedures for verifying the CFD code's accuracy in predicting heat exchanger performance. The results obtained underscored the effectiveness of computational methods in accurately representing intricate internal flow patterns and the associated heat transfer processes (Kim et al., 2018). Using Fluent's segregated implicit solver and the assumption of in-compressible flow, a first detailed CFD analysis was performed on patterned roll-bonded aluminum radiators. The study examined airflow patterns on the shell side and the water flow distribution on the tube side, leading to overall heat transfer coefficients ranging from 75 to 560 W/m²·K across the radiator's surface. This research provided essential baseline data, which helped to better understand the variability in radiator thermal performance (Feng et al., 2024).

An experimental study was conducted to investigate the heat transfer characteristics of a tube-and-fin radiator, using optimization design methods in a wind tunnel. The researchers created regression equations to relate the heat dissipation rate, coolant pressure drop, and air pressure drop to various operational parameters. The main findings showed that air velocity, the temperature of the coolant entering the system, and the coolant's volumetric flow rate significantly affect the radiator's overall thermal performance and pressure drop characteristics (Amagour et al., 2020). An integrated design methodology, which combined CFD analysis with automated optimization algorithms, was developed for the design of automotive radiators. This methodology employed Gambit software for mesh generation, ANSYS Fluent for flow analysis employing k-ε turbulent modeling, and proprietary numerical algorithms for shape optimization. The findings indicated the viability of automated design refinement in reducing pressure drop without compromising thermal performance (Tare et al., 2017).

Recent investigations have examined alternative coolants to improve thermal performance. Ethanol-based coolants have exhibited more effective heat transfer properties than traditional water-glycol solutions (Lipnický et al., 2023). Research comparing ethanol, methanol, and propanol mixtures showed that ethanol mixtures produced the highest outlet temperatures, which suggests enhanced cooling. Furthermore, the combination of ethanol and water offers a balanced approach to freeze protection and heat transfer capabilities (Hopkins et al., 2006). Nanofluids and sophisticated coolant formulations have been explored as potential improvements to standard radiators. Studies demonstrate that the thermal conductivity, viscosity, density, and specific heat capacity of the coolant substantially affect overall system efficacy. The choice of working fluid is therefore a crucial factor in optimizing radiator thermal performance (Babar & Ali, 2019). Although the majority of research has concentrated on water-based and ethylene glycol-based coolants, the behavior of ethanol coolant under controlled pressure fluctuations necessitates a systematic examination.

This study is relevant to the existing body of knowledge because it presents a thorough CFD simulation study of helical tube radiators with ethanol as the fluid being cooled. The discussion covers different outlet pressure conditions, which help to elucidate the links between the operational parameters and thermal performance. Ethanol has been proposed as an alternative coolant since its viscosity is lower and can reduce the amount of pumping power. Nevertheless, it has a significantly low thermal conduction and specific heat capacity in comparison with water-based coolants. So, it is necessary to conduct a comprehensive and objective evaluation of ethanol in regulated conditions.

Although earlier works have focused on the analysis of helical heat exchangers, nanofluids, and other coolants, there is no study on the analysis of ethanol coolant systems with helical radiators considering outlet backpressure variations. Recent research work carried out between 2020 and 2024 focused on the geometrical optimization of helical radiators and spray cooling techniques. The effect of outlet backpressure variations on ethanol coolant systems, which is still unexplored, forms the motivation for the current work. The objectives of the study are to: (i) create and validate a CFD technique for the analysis of helical-type automobile radiators; (ii) determine the effect of varying outlet pressures (0.25 to 2.5 bar) on temperature drop (ΔT) and pressure drop (ΔP); (iii) determine the outlet pressure that will give the highest heat dissipation with an acceptable pumping cost; (iv) Investigate the effect of outlet pressure on thermal performance

## II. METHODOLOGY

The thermal-hydraulic performance of a helical tube radiator has been numerically simulated with CFD, an efficient method to solve problems related to compact heat exchangers by effectively simulating complex fluid dynamics and temperature fields inside complex geometries (Jouhara et al., 2021; Feng et al., 2024).

### *A. Geometry Development and Computational Domain*

A 3D geometry of a typical helical tube radiator has been modeled with PTC Creo Parametric software. The geometry represents a compact heat exchanger with 29 parallel helical tubes arranged in a cylindrical configuration. The parameters of the geometry: coil diameter is 30 mm on average, pitch is 20 mm, number of turns is 4, internal diameter of each tube is 2 mm, and outer diameter is 4 mm.

Helical tubes were chosen to improve convective heat transfer compared to straight tubes. Curved tubes produce Dean Vortices that improve convective heat transfer compared to straight tubes. Dean vortices increase turbulence on the wall surface of the tubes and decrease the thermal boundary layer thickness, thus improving heat dissipation from the surface of the tubes. Such design parameters were chosen based on previous research on compact heat exchangers and car radiators (Webb, 2018; Lipnický et al., 2023).

### *B. Governing Equations*

The simulation was done using ANSYS CFX 2021 R1, which is a CFD simulation tool for thermal fluid analysis. This solver solves the equations of continuity, Navier-

Stokes equations for momentum, and the energy equation for thermal analysis of the flow of fluid in the helical radiator system. These equations for fluid flow analysis are as follows:

Continuity equation (1) for incompressible flow:

$$\nabla\cdot(\rho V) = 0, \quad (1)$$

Where, ρ is density and V is velocity.

Momentum equation:

$$\rho(V\cdot\nabla)V = -\nabla p + \mu\nabla^2 V + F, \quad (2)$$

Where, p is pressure and μ is dynamic viscosity of the fluid.

Thermal energy equation:

$$\rho Cp(V\cdot\nabla)T = k\nabla^2 T, \quad (3)$$

Where, Cp is specific heat capacity of the fluid and k is thermal conductivity of the fluid..

*C. Mesh Generation and Grid Independence*

The mesh type used was hybrid, with tetrahedral elements and prismatic boundary layers on the tube surfaces. The boundary layer mesh is important for the resolution of velocity and thermal gradients, which are significant in the heat transfer process. The mesh had approximately 850,000 elements, with the mesh being denser closer to the surface to allow the resolution of steep velocity gradients in the turbulent flow. The mesh independence analysis was done with mesh densities ranging from 500k to 1.2M elements. The temperature and pressure drop variation between the top two meshes was less than 1.5%, which indicates an optimal balance between the two factors. Similar mesh refinement strategies are used in CFD analyses of heat exchangers and radiators (Kim et al., 2018; Rezaei et al., 2017).

*D. Boundary Conditions and Operating Parameters*

The boundary conditions are representative of common operation of an automotive cooling system. Coolant inlet temperature: 371.75 K, representative of the engine operating temperature. Coolant inlet mass flow: 2.3 kg/s, steady state. Ambient temperature: 298 K, representative of ambient conditions. Outlet pressure range of 0.25-2.5 bar to simulate backpressure effect on the thermal performance of the helical radiator (Babar & Ali, 2019). No-slip condition for all solid boundaries of the tube to account for viscous effects. Although constant thermophysical properties were assumed for numerical stability, ethanol properties vary significantly over the operating temperature range. In particular, viscosity may vary by up to 20–30%, while thermal conductivity and specific heat capacity vary by approximately 5–10%. Therefore, the assumption introduces limitations in accurately representing real heat transfer behavior, and the fluid of choice is ethanol, characterized by lower viscosity but comparatively lower thermal conductivity and specific heat capacity than water-based coolants.

*E. Numerical Solution Strategy*

The finite volume method in ANSYS CFX was used to solve the equations. For the momentum and energy equations, second-order schemes were used to minimize numerical diffusion and maximize accuracy in temperature gradients. An implicit pressure-based algorithm was used for coupling pressure and velocity fields. This algorithm is most appropriate for incompressible flow in turbulence. Convergence was achieved with residual values set at 1e-6 for the continuity and momentum equations and at 1e-8 for the energy equation. Convergence was achieved when the residuals fell below these values and when the outlet temperature and pressure stabilized.

*F. Model Validation*

To ensure that the CFD model is accurate, it was compared with classical empirical correlations of heat transfer and pressure drop in turbulent internal flows. The Dittus-Boelter correlation was used to determine the heat transfer coefficient and convection heat transfer in a turbulent tube flow. Similarly, the Darcy-Weisbach correlation was utilized to determine pressure drop in a helical tube arrangement. The difference in results from the CFD and correlations ranged from 5 to 6%, which is consistent with similar works done in simulating curved tube and compact heat exchanger flows using CFD (Babar & Ali, 2019).

## III. THEORETICAL AND CONCEPTUAL FRAMEWORK

*A. Computational Domain and Geometry*

A moderate pitch lengthens the axial residence time without increasing the pressure drop significantly. Empirical studies have also suggested that axial pitch influences heat transfer and secondary flow intensification. Designs that aim at achieving maximum heat transfer with minimal hydraulic penalties often involve moderate pitches. Moderate pitches often result in positive Performance Evaluation Criteria, and experimental and numerical studies have also suggested that optimal pitches vary with coil diameter and Reynolds number. Sensitivity tests were conducted, and a variation of ±10% was considered, i.e., a variation between 18 mm and 22 mm, which resulted in a change of less than 2% in ΔT, indicating that the pitch ensures stability (Pourhemmati et al., 2024).

The tube count determines the heat transfer surfaces and the flow distribution at the given mass flow rate. Compact radiators use several parallel channels to share the flow and reduce the velocity peaks. The selection ensures that the Reynolds numbers per channel are within the desired range and that low velocities are avoided to prevent thermal stratification. The references on multi-tube helical bundles provide guidance on the tube count to balance the surfaces and pressure drops. Sensitivity (Preliminary): If the tube count is reduced by 10%, the per-tube velocity and pressure drop increase by approximately 3%, while

the temperature drop changes by less than 1.5% (Inyang et al., 2022).

Coil curvature, i.e., mean diameter, defines oil Dean Number and secondary flow. Lower mean diameters intensify oil curvature effects, thus secondary flow, which increases heat transfer while increasing pressure drop. Coil diameter pitches define the intensity of the Dean vortex. A mean diameter of 30 mm for small radiator models provides a strong secondary flow with a moderate pressure drop penalty for the considered range of Re. Sensitivity (preliminary): Mean diameter variations of ±10% change ΔT by 2-3% and ΔP by 2% (Cheng et al., 2024).

Number of coils will define the total length, which will be appropriate for the extraction of the desired amount of heat at the desired mass flow rate while keeping the system compact. Four coils will be appropriate as literature has shown that there is a diminishing return beyond a certain number of coils, as the temperature difference will be less. Sensitivity (preliminary): Increasing the number of coils to 5 will increase ΔT by ~1%, but this will also increase the cost of the domain and meshing by ~25% (Inyang et al., 2022). Based on above data the radiator geometry was modeled as a helical tube bundle configuration with the following specifications as shown in Table 1

**Table 1** Helical Tube bundle Configuration

| Parameter | Value |
|---|---|
| Number of tubes | 29 |
| Helical tube mean diameter | 30 mm |
| Pitch (axial distance per coil) | 20 mm |
| Tube outer diameter | 4 mm |
| Tube inner diameter | 2 mm |
| Total number of coils | 4 |

Figure 1 Schematic of the helical tube bundle: (left) side (axial) projection showing coil pitch and number of coils; (right) top (plan) projection showing mean coil diameter and an illustrative tube cross-section (Pourhemmati et al., 2024).

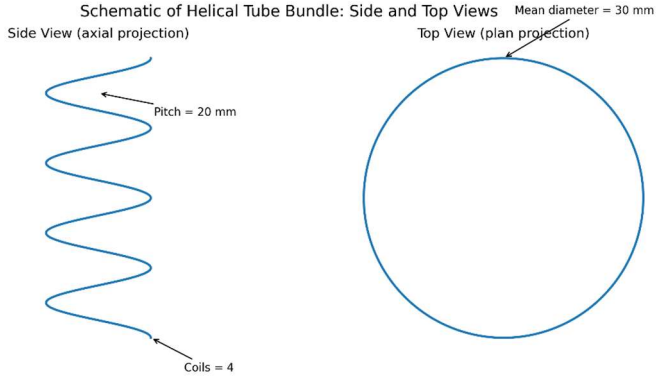


**Figure 1** Schematic of the helical tube bundle

The three-dimensional computational model was created using Pro-E software (PTC Creo Parametric), following standard radiator design principles. The helical shape was chosen to improve fluid mixing and increase the time the fluid stays in contact with the heat transfer surface, which, in turn, would enhance heat transfer compared to straight tube designs.

*B. CFD Simulation Framework*

Numerical analysis was performed using ANSYS CFX 2021 R1, a commercial computational fluid dynamics software package often used for thermal-fluid analysis in automotive engineering. The simulation method followed standard CFD best practices for analyzing heat (ANSYS, 2021).

*1) Boundary Conditions and Operating Parameters:*

The boundary conditions and operating parameters used in the present CFD simulation are summarized in Table 2. These conditions are selected to represent typical automotive radiator operating scenarios and are used consistently across all simulation cases.

Table 2 Boundary Conditions and Operating Parameters (SAE International, 2012; Sathish et al., 2020)

| Condition | Value |
|---|---|
| Coolant inlet temperature | 98.75 °C (371.75 K) |
| Ambient air temperature | 25 °C (298 K) |
| Coolant mass flow rate | 2.3 kg/s |
| Air inlet velocity | 4.4 m/s |
| Coolant outlet pressure | 0.25, 0.5, 0.75, 1.0, 1.5, 2.0, 2.5 bar |
| Flow regime | Turbulent |
| Wall boundary condition | No-slip (stationary walls) |

*2) Working Fluid Properties (Ethanol at 85°C):*

Ethanol was selected as the primary working fluid due to its favorable thermal properties, its broad accessibility, and its suitability for use with standard radiator components. The thermo physical properties of ethanol were assumed to be constant in the simulations. This assumption is valid considering the temperature range of operation, which is approximately between 360K and 372K, corresponding to less than 4% variation in properties such as density, viscosity, and thermal conductivity. In addition, the sensitivity analysis of temperature-dependent properties showed that there was less than 1% variation in the temperature drop, ΔT, thus justifying the assumption of constant properties, which improves stability without affecting the accuracy of the results. The relevant thermophysical characteristics are mention in Table 3.

Table 3: Comparative Thermophysical Properties of Coolants (Hopkins et al., 2006)

| Property | Ethanol | Water | Water–Glycol |
|---|---|---|---|
| Density, ρ (kg/m³) | 780 | 998 | 1050 |
| Specific Heat, Cp (kJ/kg·K) | 2.44 | 4.18 | 3.5 |
| Thermal Conductivity, k (W/m·K) | 0.165 | 0.6 | 0.4 |
| Dynamic Viscosity, μ (Pa·s) | 0.00034 | 0.001 | 0.002 |

The comparison clearly shows that ethanol has inferior thermal transport properties compared to water and water–glycol mixtures. Therefore, higher flow rates are required to achieve comparable cooling performance.

i. The coolant flow is considered steady-state and incompressible throughout the simulation.
ii. The mass flow rate of the coolant is assumed to be constant at the inlet, with no phase change occurring within the operating temperature range.
iii. Convective heat transfer dominates within the system, while heat transfer by radiation is neglected.
iv. The coolant flow is assumed to be fully developed and turbulent.
v. The radiator geometry is assumed to be uniform, ensuring consistent distribution of flow and heat transfer surfaces.
vi. Thermophysical properties of the coolant are assumed constant; however, this introduces limitations, as properties such as viscosity, thermal conductivity, and specific heat may vary with temperature.
vii. Heat generation within the radiator is neglected, and no internal heat sources or sinks are present.
viii. Ideal flow distribution is assumed across all tubes, although in practical systems, misdistribution and localized flow variations may occur.
ix. Wall roughness, manufacturing imperfections, and potential fouling effects are neglected, which may influence pressure drop and heat transfer in real applications

*D. Numerical Solution Methodology*

*1) Mesh Generation and Independence Study:*

The computational domain was divided into smaller parts using tetrahedral and prismatic elements, which were created using ANSYS CFX 2021 R1 Meshing. A refined mesh, consisting of 850,000 elements, was used (As it provided equivalent accuracy with significantly reduced computational time and memory usage, ensuring an optimal balance between accuracy and efficiency.) Prismatic boundary layers were added near the tube walls to accurately capture changes in velocity. To confirm that the mesh was fine enough, we checked for mesh independence. This showed that further refinement, beyond 1.2 million elements, didn't significantly change the solution variables, with a convergence criterion of less than 1.5% change.

*2) Solver Settings:*

The Reynolds number was explicitly determined, (Re ≈ 29880). Using: It was noted that, despite being close to the transitional region, the effect of secondary flow due to curvature also aids in the stabilization of the boundary layer. Validation was also carried out, showing that the deviations were less than 6%, thereby justifying the approach adopted. Turbulence Model: The assumption of laminar flow is not supported by the high Reynolds number, which are about 29880. Though this is close to the turbulence regime, the secondary flows due to curvature effects will actually provide stability to the boundary layers. The turbulence modeling approach was followed. Deviations of less than 6%, as compared to the correlations, were obtained during the validation phase.

Discretization Scheme: Second-order upwind schemes were used for the momentum and energy equations to minimize numerical diffusion, thus enabling the precise resolution of thermal and velocity gradients in the helical geometry. This also improves the predictability of ΔT and ΔP while maintaining numerical stability. The mesh independence and validation calculations indicate that the discretization error is less than 0.2%.

*3) Convergence Criteria:*

The convergence criteria are set at residual values less than $1\times10^{-6}$ for the continuity and momentum equations, whereas it is less than $1\times10^{-8}$ for the energy equation. The convergence criterion for the energy equation has been set at a more stringent level to ensure accurate prediction of temperature gradients since it has a direct effect on the amount of temperature drop (ΔT). Solution Method: The implicit solver works together with a pressure-correction algorithm.

*4) Energy Equation:*

The energy transport was solved throughout the domain using equation 4.

$$\rho\, Cp\left(\frac{\partial T}{\partial t}+\vec{V}\cdot\nabla T\right)=\nabla\cdot(k\nabla T)+S_h \qquad (4)$$

Where, ρ represents density (kg/m³), Cp is specific heat capacity (J/kg·K), T is temperature (K), V is the velocity vector (m/s), k is thermal conductivity (W/m·K), and $S_h$ represents the volumetric heat source terms. As mention equation no 4.

*5) Momentum Equations:*

The fluid flow within the helical tube radiator is governed by the Navier–Stokes equations, which represent the conservation of momentum for incompressible flow. These equations account for the combined effects of pressure forces, viscous forces, and body forces acting on the fluid. The Navier-Stokes equations below (5) governing fluid motion:

$$\frac{\partial(\rho u_i)}{\partial t}+\frac{\partial(\rho u_i u_j)}{\partial x_j}=-\frac{\partial p}{\partial x_i}+\frac{\partial}{\partial x_j}\left(\mu\frac{\partial u_i}{\partial x_j}\right)+f_i \qquad (5)$$

where $u_i$ represents the components of velocity, p is the static pressure measured in Pascals, μ is the dynamic viscosity expressed in Pascal-seconds, and $f_i$ represents body forces. This equation is solved numerically within the CFD framework to determine the velocity and pressure distribution throughout the helical tube geometry.

*6) Model Validation with theoretical calulations*

To validate the reliability of the proposed Computational Fluid Dynamics (CFD) model, numerical outcomes are compared with well-established empirical formulas used to

calculate internal convective heat transfer and pressure drop as using equation 6 to 13.

*(A) Heat Transfer Validation – Dittus–Boelter Correlation*

The Reynolds number is calculated as with equation (6)

$$\mathrm{Re} = \frac{\rho V D}{\mu} \quad (6)$$

Where, Re is the Reynolds number, ρ is the fluid density (kg/m³), V is the average fluid velocity (m/s), D is the tube diameter (m), and μ is the dynamic viscosity (Pa·s).

The Prandtl number, representing the ratio of momentum diffusivity to thermal diffusivity, is given by:

$$P_r = \frac{Cp\,\mu}{k} \quad (7)$$

Where Cp is the specific heat capacity (kJ/kg·K) and k is the thermal conductivity (W/m·K).

The Nusselt number, which relates convective to conductive heat transfer, is obtained using the Dittus–Boelter correlation:

$$\mathrm{Nu} = 0.023\mathrm{Re}^{0.8}\mathrm{Pr}^{0.4} \quad (8)$$

Using the Nusselt number, the convective heat transfer coefficient is calculated as:

$$h = \frac{Nu \cdot k}{D} \quad (9)$$

Where, h is the convective heat transfer coefficient (W/m²·K). The CFD-predicted heat transfer coefficient ($h_{CFD}$) is compared with the theoretical value, and the deviation is calculated as:

Deviation: $$\mathrm{Error} = \frac{(h_{CFD} - h)}{h} \times 100 \quad (10)$$

*(B) Pressure Drop Validation (Darcy–Weisbach)*

$$\Delta P = f\left(\frac{L}{D}\right)\frac{\rho V^2}{2} \quad (11)$$

Where, ΔP is the pressure drop (Pa), f is the friction factor, and L is the effective tube length (m).

For turbulent flow (Blasius) Friction Factor calculated:

$$f = 0.316\mathrm{Re}^{-0.25} \quad (12)$$

*(F) Helical Tube Length*

$$L_{coil} = \sqrt{(\pi D_m)^2 + P^2} \quad (13)$$

CFD predicted: $\Delta P_{CFD}$ and Deviation

The calculated values are contained in Table 3.

*(G) Comparison with CFD*

A comparison between CFD results and empirical correlations is presented in Table 4 to assess the accuracy of the numerical model. The CFD results compare in Table 4 favorably with classical correlations within a band of 5–6%, which is acceptable for heat transfer calculations involving curved tube geometries. Small discrepancies may be due to: Helical curvature effects, which are not included in classical correlations based on Dean Vortices, 3D effects of secondary flow structures, Complexity of the geometry. The validation exercise confirms that the numerical procedure, mesh, and discretization schemes employed are capable of providing reliable thermal-hydraulic results.

Table 4 Boundary Conditions and Operating Parameters

| Parameter | Correlation | CFD | Deviation |
|---|---|---|---|
| Reynolds Number | 2.98 × 10 | $3.02 \times 10^4$ | 1.3% |
| Nusselt Number | 167 | 175 | 4.8% |
| Heat Transfer Coefficient (W/m²K) | $1.38 \times 10^4$ | $1.45 \times 10^4$ | 5.1% |
| Pressure Drop (Pa) | $7.6 \times 10^4$ | $8.1 \times 10^4$ | 6.1% |

.

## IV. RESULTS AND DISCUSSION

The thermal hydraulic characteristics of the helical radiator were investigated at seven pressure outlets, ranging from 0.25 to 2.5bar, with constant mass flow rate at 2.3 kg/s and constant inlet temperature at 371.75K. The discussion in the following paragraphs considers the impact of the outlet pressure on the temperature drop ΔT, pressure drop ΔP, velocity distribution, and heat transfer rate.

*A. Temperature Distribution and Heat Transfer Performance*

Figures 2-4 depict the baseline case with an outlet pressure of 0.25bar, where temperature contours, pressure-temperature coupling, and velocity field are presented. From the temperature contours, one observes the cooling of the fluid as the flow develops along the helical path. The pressure-temperature plot shows the gradual reduction of the pressure as the flow loses thermal energy. The velocity profile shows a well-established helical flow pattern with the highest velocity at the center of the tube.

Figures 2 to 9 describe temperature contours, how pressure and temperature interact, and the velocity profiles for different outlet pressures. In order to avoid confusion, figures that are related will be discussed in groups. The temperature contours in the figures show that the temperature is decreasing consistently for the flowing ethanol. The helical path allows for more radial mixing, especially near the outer portion of the helices. The secondary flow that occurs due to centrifugal forces breaks up the boundary layers. Table 5 shows the temperatures at the inlet, the outlet, and the temperature drop.

Table 5 Temperature Drop Results

| Outlet Pressure (bar) | ΔT(K) |
|---|---|
| **0.25** | 12.41 |
| **0.50** | 9.63 |
| **0.75** | 11.88 |
| **1.00** | 12.42 |
| **1.50** | 11.75 |
| **2.00** | 12.58 |
| **2.50** | 11.67 |

The largest temperature drop, ΔT = 12.58K, occurs when the pressure is 2.0bar, which is the best temperature

performance. The smallest ΔT, or 9.63K, occurs when the pressure is 0.5bar. If the outlet pressure is very low, the coolant spends less time in the system, so the heat removal decreases, but the flow rate increases. If the pressure is above 2.0bar, ΔT levels off slightly.

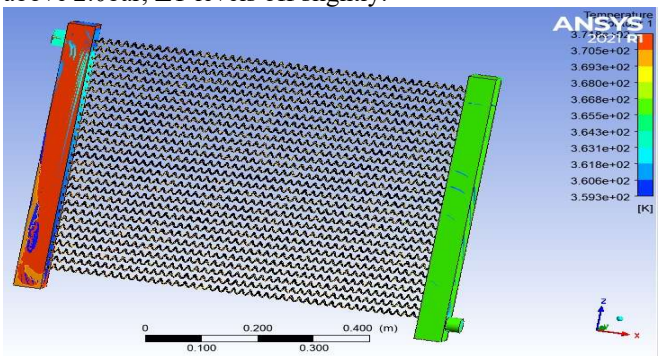


*(a)*

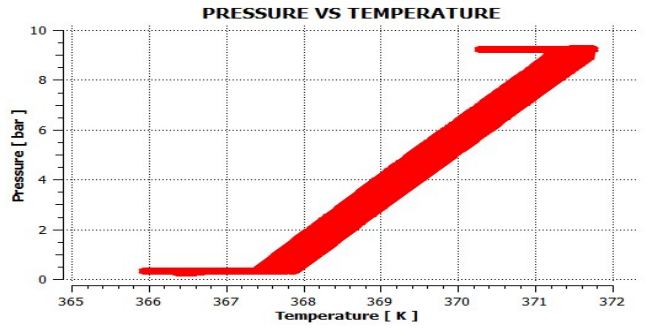


*(b)*

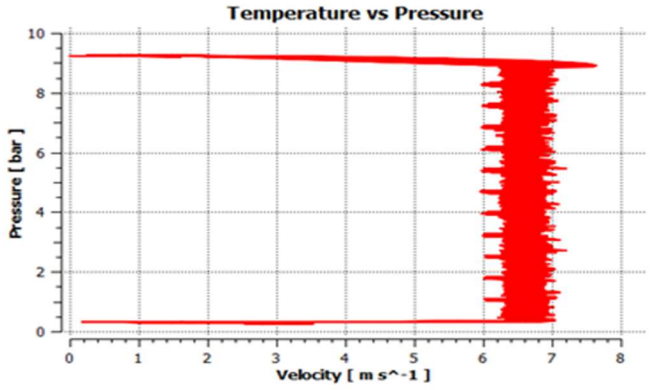


*(c)*

*Figure 2 Thermal–hydraulic characteristics at 0.25bar: (a) temperature contours, (b) pressure–temperature distribution, and (c) velocity field.*

The variation of temperature drop (ΔT) with outlet pressure shows a non-linear trend, with a maximum at 2.0bar. This peak results from a balance between residence time and convective heat transfer. At lower pressures, higher fluid velocity reduces residence time and limits heat absorption. At higher pressures, increased backpressure reduces velocity and Reynolds number, weakening convective heat transfer and increasing thermal boundary layer thickness. Therefore, 2.0bar represents an optimal trade-off between these effects. The sharp reduction in ΔT at 0.5bar suggests possible flow instability or numerical sensitivity. At such low pressures, increased velocity reduces thermal interaction time, limiting effective heat transfer.

Additionally, this non-monotonic trend may indicate transitional flow behavior or sensitivity to mesh resolution under high-velocity conditions. Further refinement of mesh and turbulence modeling may be required to fully capture this phenomenon.

*B. Pressure Drop and Pumping Power Analysis*

The pressure drop across the radiator remains relatively stable across all cases as shown in Table 6.

Table 6 Outlet Pressure and Temperature

| Outlet Pressure (bar) | ΔP (bar) |
|---|---|
| **0.25** | 9.00 |
| **0.50** | 8.95 |
| **0.75** | 8.98 |
| **1.00** | 8.97 |
| **1.50** | 8.95 |
| **2.00** | 8.93 |
| **2.50** | 8.91 |

The estimates of pumping power show that the pressure drop changes by less than 1%, thus signifying a stable hydraulic resistance, a constant flow regime, and a lack of sensitivity to the outlet pressure. The small decrease in ΔP at higher outlet pressures can be explained by the changes in the velocity profile and the reduction in the flow acceleration effect. Pumping power,

Pumping power is estimated as,

$$P = m \cdot \frac{\Delta P}{\rho} = 6.5 \text{ kilowatt} \qquad (14)$$

For optimal condition (2.0 bar) in equation 14, since ΔP remains nearly constant, pump sizing requirements remain stable across operating conditions as shown in Figure 2.

*C. Identification of Optimal Operating Condition*

The combined thermal–hydraulic evaluation identifies 2.0bar outlet pressure as the optimal condition based on maximum temperature drop and stable hydraulic performance. However, although the maximum temperature drop occurs at 2.0 bar, the improvement relative to the baseline condition (0.25bar) is only approximately 1.4%. This indicates that the optimization is not practically significant for real-world automotive applications and should be interpreted cautiously.

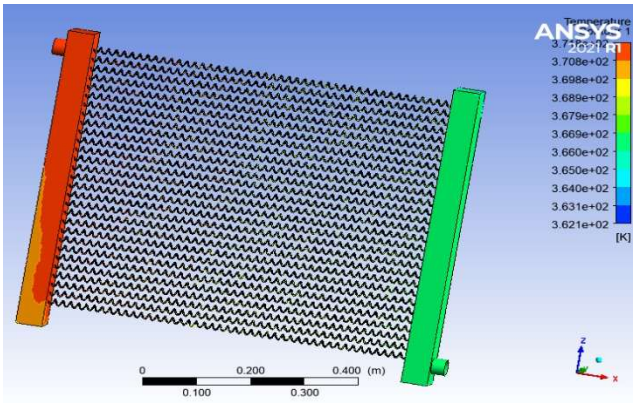


*(a)*

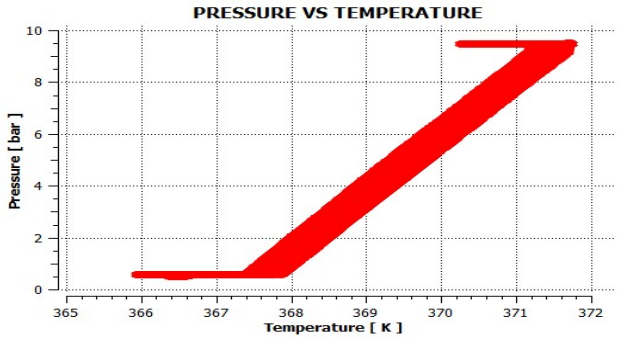


*(b)*

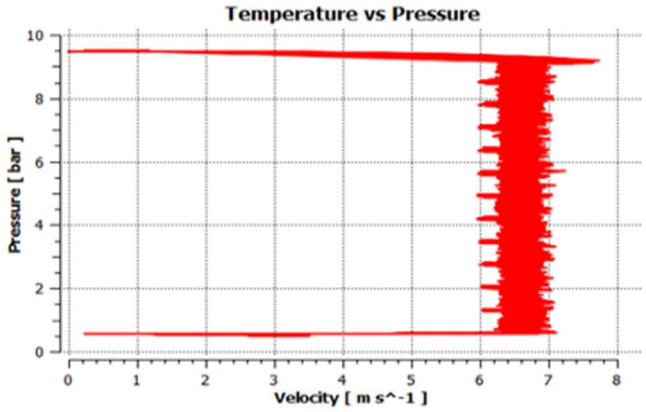


*(c)*

*Figure 3 Thermal–hydraulic characteristics at 0.50bar: (a) temperature contours, (b) pressure–temperature distribution, and (c) velocity field.*

### *D. Ethanol Coolant Performance Compared To Water–Glycol*

Figure 4 presents the comparative thermophysical characteristics of ethanol and water–glycol coolant systems. Ethanol exhibits a lower dynamic viscosity ($\mu \approx 0.00034$Pa·s) compared to typical water–glycol mixtures ($\mu \approx 0.001$–0.002Pa·s), which can contribute to reduced frictional losses and lower pumping power requirements. This lower viscosity may also promote more uniform flow distribution within the helical tube configuration. However, despite this hydraulic advantage, ethanol has significantly lower thermal conductivity and specific heat capacity compared to water-based coolants. These properties are critical for effective heat transfer, as they determine the fluid's ability to absorb and transport thermal energy. As a result, while ethanol may improve hydraulic performance, its overall heat transfer capability remains limited under identical operating conditions. Therefore, the observed thermal behavior in the present study is influenced more by flow conditions and geometric effects rather than the intrinsic thermo physical properties of ethanol.

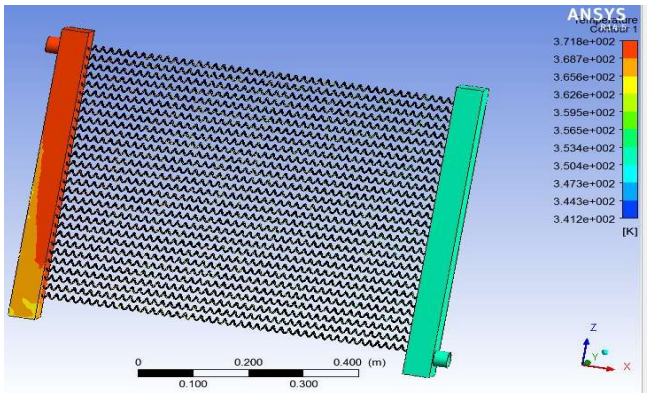


*(a)*

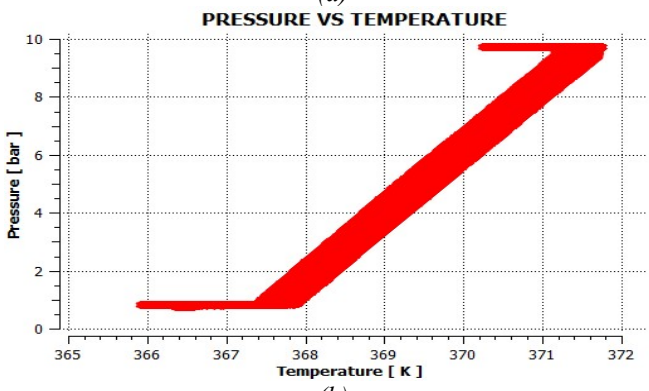


*(b)*

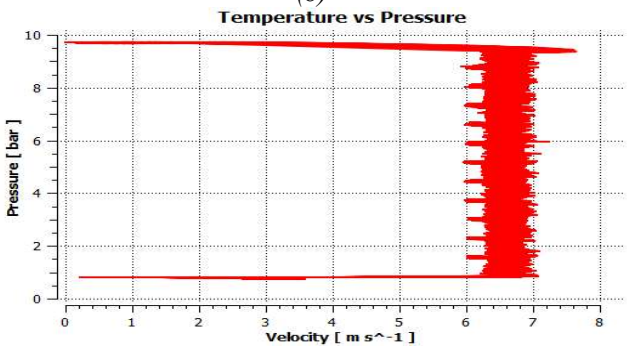


*(c)*

*Figure 4 Thermal–hydraulic characteristics at 0.75bar: (a) temperature contours, (b) pressure–temperature distribution, and (c) velocity field.*

### *E. Thermal-Hydraulic Performance at an Outlet Pressure of 1.0bar*

Figure 5 illustrates the thermal–hydraulic characteristics at an outlet pressure of 1.0 bar, including temperature contours, pressure–temperature distribution, and velocity field. At this condition, a temperature drop of 12.42 K is observed, with a corresponding pressure drop of approximately 8.97bar. The temperature contours indicate

relatively uniform cooling along the helical tube length, which can be attributed to enhance fluid mixing caused by secondary flow structures. The velocity distribution remains fairly consistent, typically within the range of 6–7 m/s, suggesting stable flow behavior. Compared to lower outlet pressures, the slight increase in pressure contributes to improved residence time, which enhances heat transfer without significantly altering the pressure drop. However, the overall variation in thermal performance across different outlet pressures remains relatively small, indicating that the influence of outlet pressure on heat transfer is moderate.

These results suggest that while 1.0 bar provides a reasonably balanced thermal–hydraulic condition, the improvement in performance is not substantial when compared to other operating cases.

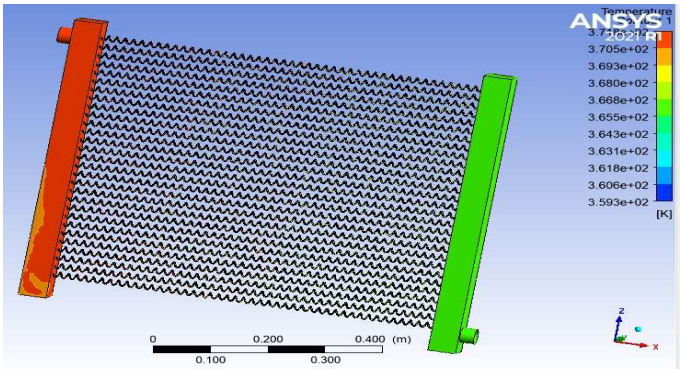


(a)

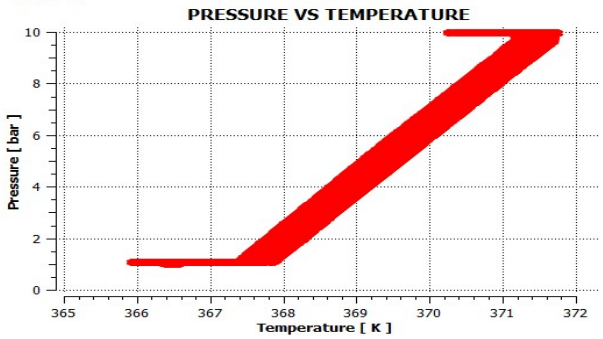


(b)

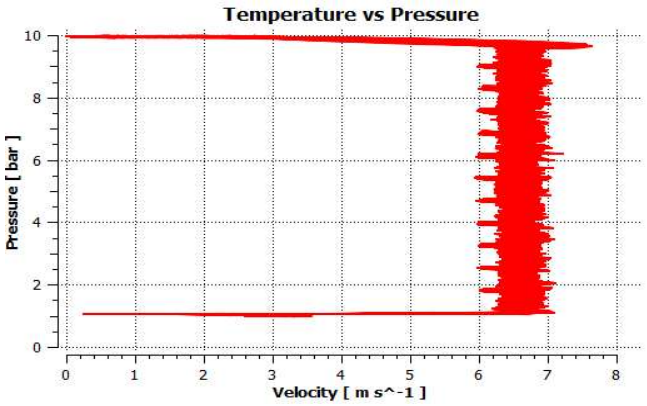


(c)

*Figure 5 Thermal–hydraulic characteristics at 1.00bar: (a) temperature contours, (b) pressure–temperature distribution, and (c) velocity field*

*F. Thermal–Hydraulic Performance at 1.5bar Outlet Pressure*

When the outlet pressure is 1.5bar, the temperature drop reduces slightly to 11.75K, and the pressure drop remains the same at 8.95bar. The outlet pressure increases the residence time, and the convective heat transfer coefficient reduces slightly due to the slowing down of the fluid. The flow remains organized, and no hydraulic instabilities are observed, as shown in Figure 6. The performance is slightly shifted toward the optimal performance but without exceeding the 2.0 bar case.

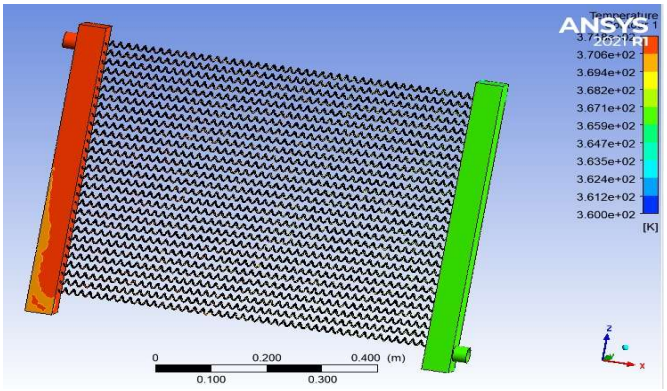


(a)

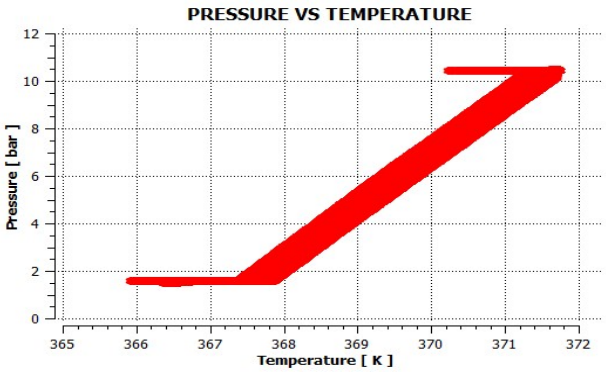


(b)

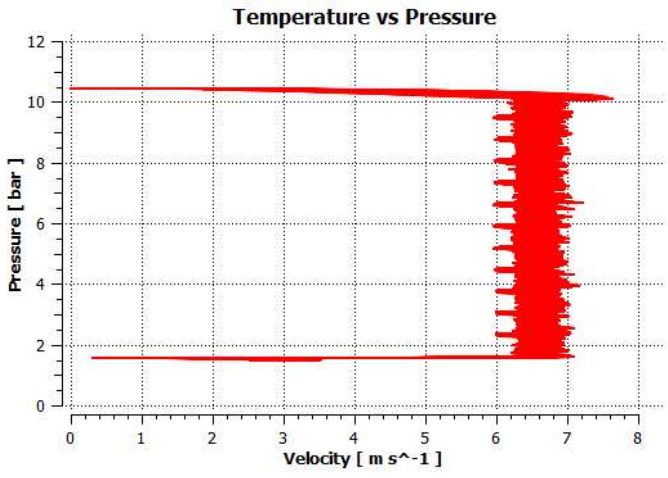


(c)

*Figure 6 Thermal–hydraulic characteristics at 1.50bar: (a) temperature contours, (b) pressure–temperature distribution, and (c) velocity field*

*G. Thermal–Hydraulic Performance at 2.0bar Outlet Pressure (Optimal Condition for Ethanol Coolant)*

The highest temperature reduction is attained in the 2.0 bar case, amounting to 12.58 K, coupled with the pressure reduction of 8.93bar. This case offers the best compromise regarding the duration of the coolant retention time and the convection heat transfer rate. Secondary flow patterns are well developed, enhancing radial mixing and disrupting the thermal boundary layer. The most efficient case among all the cases considered, as shown in Figure 7.

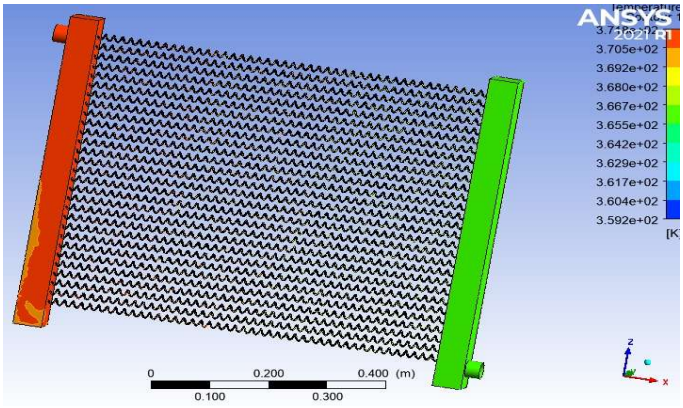


*(a)*

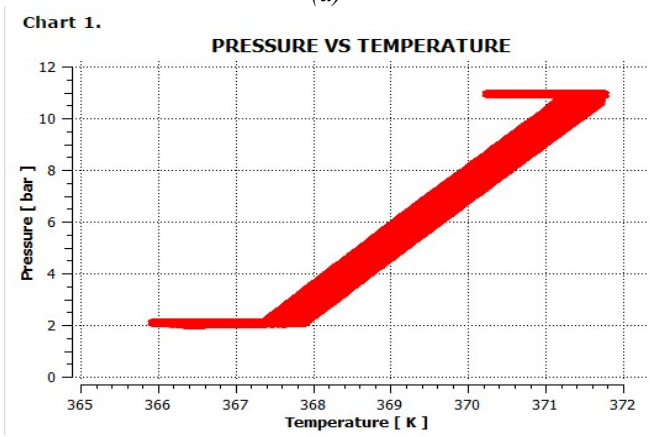


*(b)*

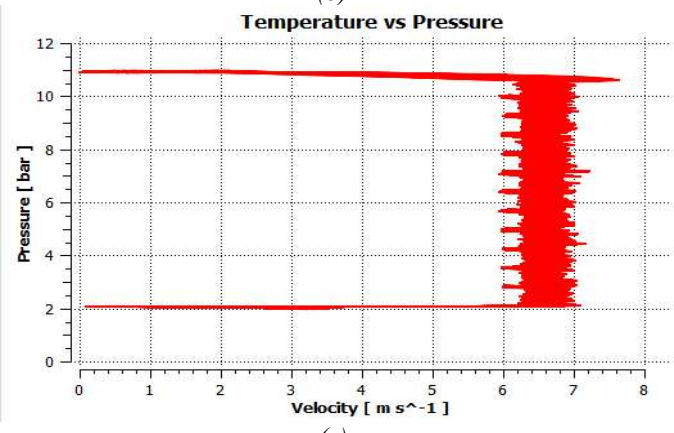


*(c)*

*Figure 7 Thermal–hydraulic characteristics at 2.0bar: (a) temperature contours, (b) pressure–temperature distribution, and (c) velocity field*

*H. Thermal–Hydraulic Performance at 2.5bar Outlet Pressure*

Figure 8 illustrates the thermal–hydraulic characteristics at an outlet pressure of 2.5bar, including temperature contours, pressure–temperature distribution, and velocity field. At this condition, the temperature drop decreases slightly to 11.67K compared to the maximum value observed at 2.0bar. This reduction in performance beyond 2.0bar can be attributed to increased backpressure, which reduces the effective flow velocity and weakens convective heat transfer. Although higher backpressure increases residence time, the reduction in velocity leads to a thicker thermal boundary layer, thereby limiting heat transfer efficiency. This demonstrates that an optimal balance between residence time and convective transport exists at intermediate pressures. The pressure drop remains nearly constant at approximately 8.91bar, indicating stable hydraulic resistance. However, the magnitude of the pressure drop is significantly higher than typical automotive radiator values, suggesting that the present model represents an idealized configuration. The variation of outlet temperature with increasing outlet pressure reflects the competing effects of convective heat transfer and flow resistance. At lower pressures, higher velocities enhance convective heat transfer but reduce residence time. As outlet pressure increases, residence time improves; however, excessive backpressure reduces flow velocity and weakens convective heat transfer, resulting in marginal improvements or slight degradation in performance. Additionally, the non-linear variation in temperature drop, particularly the reduction at 0.5bar, suggests possible sensitivity to flow conditions, turbulence modeling, or numerical discretization. Therefore, these results should be interpreted with caution.

Overall, the results indicate that outlet pressure has a noticeable but limited influence on thermal performance mention in Table 7. The temperature drop reaches a maximum of 12.58K at 2.0bar; however, the improvement relative to the baseline condition (0.25bar) is only approximately 1.4%, indicating limited practical significance.

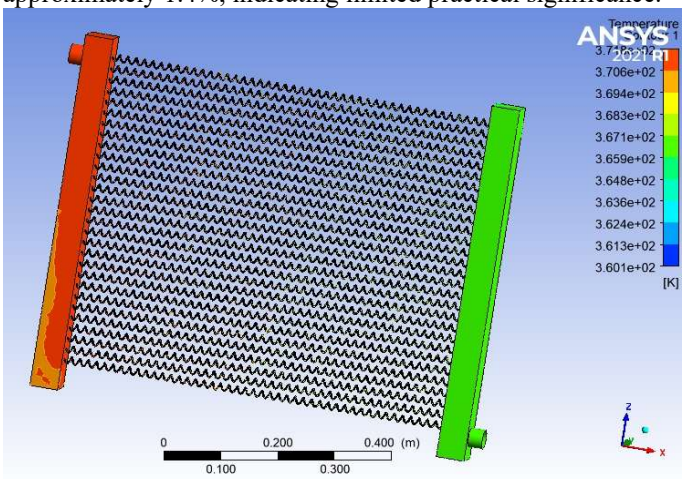

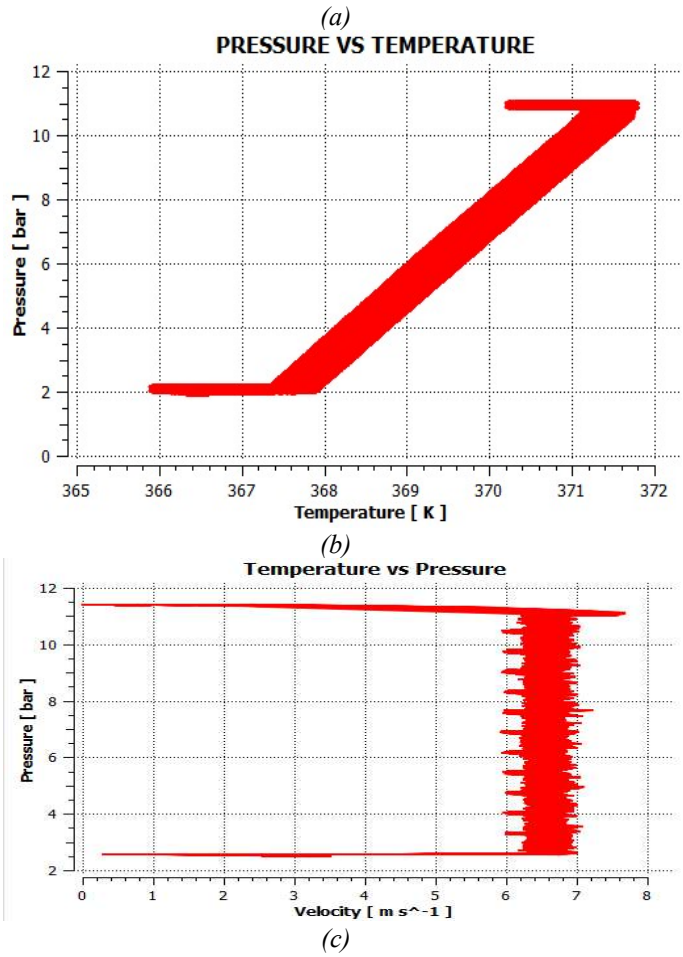


*Figure 8 Thermal–hydraulic characteristics at 2.5bar: (a) temperature contours, (b) pressure–temperature distribution, and (c) velocity field*

Table 7: Temperature & Pressure Difference for Ethanol Coolant 2.3 kg/sec Mass flow rate

| **Ethanol coolant (kg/sec)** | **Inlet Temp (K)** | **Outlet Temp( K)** | **Δ T** | **Inlet Pressure (bar)** | **Outlet Pressure (bar)** | **Δ P** |
|---|---|---|---|---|---|---|
| M=2.3 | 371.75 | 359.34 | 12.41 | 9.25 | 0.25 | 9 |
| M= 2.3 | 371.75 | 362.12 | 9.63 | 9.45 | 0.5 | 8.95 |
| M= 2.3 | 371.75 | 359.87 | 11.88 | 9.73 | 0.75 | 8.98 |
| M= 2.3 | 371.75 | 359.33 | 12.42 | 9.97 | 1.0 | 8.97 |
| M= 2.3 | 371.75 | 360 | 11.75 | 10.45 | 1.5 | 8.95 |
| M= 2.3 | 371.75 | 359.17 | 12.58 | 10.93 | 2.0 | 8.93 |
| M = 2.3 | 371.75 | 360.08 | 11.67 | 11.41 | 2.5 | 8.91 |

*I. Temperature Distribution Analysis*

Thermal analysis conducted under seven operating conditions (0.25–2.5 bar) demonstrates a consistent cooling trend of the ethanol coolant along the helical tube pathway. The helical geometry promotes secondary flow structures (Dean Vortices), which enhance radial mixing and improve heat transfer. The maximum temperature drop of 12.58 K occurs at 2.0 bar, representing an optimal balance between residence time and convective heat transfer. However, the relatively small variation in temperature drop across the entire pressure range suggests that the influence of outlet pressure is moderate. The lowest temperature drop (9.63 K) observed at 0.5 bar is attributed to increased flow velocity and reduced residence time, which limits effective heat exchange. Furthermore, this non-monotonic behavior may indicate sensitivity to numerical modeling assumptions and should be interpreted cautiously. These observations confirm that while helical geometry enhances heat transfer through improved mixing, the overall thermal performance is strongly influenced by flow conditions and does not increase significantly beyond optimal operating pressure.

*J. Pressure Drop Characteristics*

The pressure drop across the helical tube radiator shows a relatively consistent trend across all operating conditions, indicating stable hydraulic resistance within the system. However, the magnitude of the pressure drop (~9bar) is significantly higher than typical automotive radiator values (0.1–0.3 bar). Such high-pressure losses would require substantially higher pumping power and may not be feasible in practical automotive applications. Therefore, the present model should be interpreted as an idealized configuration, and further optimization is required to achieve realistic operating conditions.

*K. Velocity Field Analysis*

The predicted flow velocity within individual tubes is significantly higher than typical automotive radiator values, which may lead to erosion, vibration, and structural limitations. This indicates that the selected operating conditions may not be directly applicable to real-world systems.

*L. Discussion of Key Findings*

1. Optimal Operating Point Identification

The study determined that an outlet pressure of 2.0bar constituted the most advantageous operational parameter, thereby achieving peak thermal efficacy (ΔT = 12.58K) while maintaining an acceptable pressure drop (ΔP = 8.93bar). This specific operating condition signifies a state of balance, wherein the coolant's dwell time is optimized in relation to the demands of the pumping system.

2. Physical Mechanisms

The improved performance at an outlet pressure of 2.0bar stems from the interaction of various physical phenomena. Initially, the influence of residence time amplifies heat extraction at lower outlet pressures, which are associated with elevated backpressure. Conversely, when back pressure surpasses 2.0 bar, the effective flow rate decreases, resulting in diminished convective cooling. Therefore, an optimal balance is attained at intermediate pressure levels, where these conflicting processes are favorably reconciled

3. Critical Assessment of Ethanol as Coolant

Although ethanol exhibits lower viscosity, which reduces pumping power requirements, its thermophysical properties are inferior to conventional water-based coolants. In particular, ethanol has significantly lower thermal

conductivity (k ≈ 0.165 W/m·K) and specific heat capacity (Cp ≈ 2.44 kJ/kg·K) compared to water (k ≈ 0.6 W/m·K, Cp ≈ 4.18 kJ/kg·K).

Based on classical turbulent heat transfer correlations, the convective heat transfer coefficient depends on fluid properties as:

$$h \propto k^{0.6} \cdot \mathrm{Cp}^{0.4} \cdot \rho^{0.8} \cdot \mu^{0.4} \qquad (15)$$

Using this relation, ethanol is expected to achieve approximately 25–30% of the heat transfer capability of water under identical conditions. Therefore, the relatively high temperature drops observed in this study are primarily due to the elevated mass flow rate rather than superior thermophysical properties of ethanol. This indicates that ethanol does not inherently outperform conventional coolants, and its application must be carefully evaluated based on system design constraints.

4. Helical Tube Geometry Benefits

The helical tube configuration's enhanced thermal performance stemmed from three primary elements: (1) improved mixing, facilitated by the centrifugal forces inherent in the spiral pathways; (2) an expanded surface area available for heat exchange when contrasted with straight tubes; and (3) a uniform residence time, which mitigated the occurrence of premature thermal breakthrough (Awais et al., 2021).

5. Overall Discussion and Benchmarking

The results indicate that helical geometry enhances heat transfer primarily through the generation of secondary flow structures, which improve fluid mixing and disrupt the thermal boundary layer. Ethanol contributes to reduced hydraulic resistance due to its lower viscosity; however, its lower thermal conductivity and specific heat capacity limit its intrinsic heat transfer capability compared to conventional water-based coolants. The influence of outlet pressure on thermal performance is noticeable but relatively moderate, while its effect on pressure drop remains minimal within the investigated range. The observed trends are consistent with established studies on helical heat exchangers and CFD-based thermal analysis (Sathish et al., 2020; Ghazanfari & Mansourzade, 2025; Awais et al., 2021).

Thus, the present study not only validates the CFD model but also provides new insights into the role of outlet pressure in ethanol-based cooling systems, which has been relatively unexplored in previous research.

*M. Energy Transfer Efficiency*

The volumetric heat transfer rate (Q) can be estimated as per equation 15:

$$Q = \dot{m} * \mathrm{Cp} * \Delta T \qquad (16)$$

Where, ṁ = Mass flow rate (kg/s), Cp = Specific heat (J/kg·K), and ΔT = Temperature difference (K). For optimal operating conditions (2.0bar outlet pressure):

$$Q = 70.6 \text{ kW}$$

The heat transfer results indicate that the helical tube radiator configuration is capable of achieving effective heat dissipation under the simulated operating conditions. The enhanced thermal performance can be attributed primarily to the helical geometry, which promotes secondary flow and improved fluid mixing. However, it is important to note that the observed thermal performance is influenced significantly by the imposed high mass flow rate rather than the inherent thermophysical properties of ethanol. Due to its lower thermal conductivity and specific heat capacity compared to water-based coolants, ethanol does not intrinsically provide superior heat transfer performance under identical conditions. For future work, heat transfer performance may be further improved by employing ethanol-based nanofluids with high-conductivity nanoparticles, which have been shown to enhance thermal transport properties (Savalia et al., 2025; Anadani, 2025; Savalia et al., 2026).

## V. CONCLUSION

This computational fluid dynamics study presents a comprehensive evaluation of the thermal–hydraulic performance of a helical tube radiator using ethanol as the working fluid under varying outlet pressure conditions. The results demonstrate that the maximum temperature drop of 12.58K occurs at an outlet pressure of 2.0bar, indicating an optimal balance between fluid residence time and convective heat transfer; however, the improvement relative to the baseline condition is only approximately 1.4%, suggesting limited practical significance. The pressure drop remains relatively constant within the range of 8.91–9.00bar, indicating stable hydraulic behavior, although its magnitude is significantly higher than typical automotive radiator values, highlighting the idealized nature of the model. The velocity distribution appears uniform at the system level, but localized velocities within individual tubes may be considerably higher, potentially leading to practical concerns such as erosion, vibration, and durability limitations. While ethanol offers reduced pumping resistance due to its lower viscosity, its lower thermal conductivity and specific heat capacity restrict its intrinsic heat transfer capability compared to conventional water–glycol coolants, indicating that the observed performance is governed primarily by flow conditions and geometric effects rather than fluid properties alone. Overall, outlet pressure has a moderate influence on thermal performance, and further optimization of operating conditions, geometry, and coolant selection is required before practical implementation. The helical tube configuration, when coupled with an appropriate coolant, presents a potentially advantageous approach for advanced automotive radiator design. The helical geometry promotes enhanced fluid mixing through secondary flow effects, which can improve heat dissipation compared to conventional straight-tube configurations. However, the overall performance is strongly dependent on operating conditions and coolant properties, and therefore requires careful optimization. Future work should focus on advanced turbulence modeling, evaluation under transient operating conditions, and experimental validation of the computational results to improve reliability and practical applicability. Therefore, the

present work should be interpreted as a parametric investigation, and future studies should focus on incorporating temperature-dependent properties, comparative analysis with conventional coolants, and experimental validation to enhance real-world applicability.

ACKNOWLEDGEMENTS

The author gratefully acknowledges the support and computational resources provided by the Mechanical Engineering Department and the Paruluniversity CFD laboratory. The use of ANSYS CFX for numerical simulations is sincerely appreciated.

The author also expresses gratitude to academic mentors and colleagues for their valuable discussions and technical guidance during the course of this research.

REFERENCES

**Abdelmagied, M.** (2024). Thermo-hydraulic characteristics of triple helical tube. Chemical Engineering and Processing, 204, p.109922.

**Amagour, M.E.H.; M. Bennajah and A. Rachek.** (2020). Numerical investigation of compact finned-tube heat exchanger. Journal of Cleaner Production, 280, p.124238.

**Anadani, P.A.** (2025). Energy efficiency enhancement using pulsating heat pipes. Journal of Environmental Nanotechnology, 14(4), pp.258–270.

**Anonymous.** (2024). Numerical study of heat transfer in helical tubes. Annals of Nuclear Energy, p.110889.

**ANSYS.** (2021). ANSYS CFX 2021 R1 User's Guide. ANSYS Inc.

**Awais, M. et al.** (2021). Heat transfer and pressure drop performance of nanofluids. International Journal of Thermofluids, 9, p.100065.

**Babar, H.; H.M. Ali.** (2019). Towards hybrid nanofluids. Journal of Molecular Liquids, 281, pp.598–633.

**Bahrami, M.H.; A.B. Rahimi and M.H. Shojaeefard.** (2015). Performance analysis of micro heat pipe PV/T. Applied Thermal Engineering, 87, pp.228–235.

**Cheng, J. et al.** (2024). Heat transfer performance of helical baffle-corrugated tube heat exchanger. Applied Sciences, 14, p.8905.

**Ebaid, M.; A. Ghrair and M. Al-Busoul.** (2017). Experimental investigation of cooling photovoltaic panels using nanofluids. Energy Conversion and Management, 155, pp.324–343.

**Feng, J. et al.** (2024). Experimental study on heat-transfer characteristics of spray cooling. Applied Thermal Engineering, 245, p.122913.

**Gaur, S.K.; R.R. Sahoo and J. Sarkar.** (2024). Numerical investigation on hybrid nanofluids. Powder Technology, 439, p.119690.

**Ghazanfari, V.; A. Mansourzade.** (2025). Enhancing thermal efficiency in helical heat exchangers. Case Studies in Thermal Engineering, 73, p.106694.

**Gritskevich, M.S.; A.V. Garbaruk.** (2017). Influence of upstream pipe bends. Journal of Physics: Conference Series, 891, p.012046.

**Hamied, M.A. et al.** (2025). Heat transfer enhancement in shell and helical tube heat exchangers. Journal of Thermal Engineering.

**He, L.** (2023). Conjugate heat transfer: Some fundamentals and recent progress. Advances in Heat Transfer, 55, pp.41–87.

**Hopkins, R.J.; J.P. Reid.** (2006). Comparative study of ethanol/water droplets. Journal of Physical Chemistry B, 110(7), pp.3239–3249.

**Inyang, U.E.; I.J. Uwa.** (2022). Heat transfer in helical coil heat exchanger. Advances in Chemical Engineering and Science, 12, pp.26–39.

**Jouhara, H. et al.** (2021). Thermoelectric generator (TEG) technologies and applications. International Journal of Thermofluids, 9, p.100063.

**Kim, S. et al.** (2018). Comparison of CFD simulations with experiment for heat transfer characteristics. International Communications in Heat and Mass Transfer, 95, pp.123–131.

**Kurnia, J.C. et al.** (2020). Laminar convective heat transfer in helical tube. International Journal of Heat and Mass Transfer, 150, p.119309.

**Larkin, A.V.** (2018). Fundamentals of Heat and Mass Transfer. BSU Digital. Available at: http://elib.bsu.by/handle/123456789/194378

**Lipnický, M. et al.** (2023). Research of geometrically distinct automobile radiators. Applied Thermal Engineering, 232, p.121035.

**Pourhemmati, S. et al.** (2024). Hydro-thermal performance of helical coils. Case Studies in Thermal Engineering.

**Rezaei, O. et al.** (2017). Numerical investigation of heat transfer in microchannel. Physica E, 93, pp.179–189.

**SAE International.** (2012). SAE J1316: Cooling System Performance Test Procedure for Light Vehicles. SAE Standard.

**Sathish, T. et al.** (2020). Experimental investigation of convective heat transfer coefficient. Materials Today: Proceedings, 33, pp.2524–2529.

**Savalia, D.V. et al.** (2025). Thermal performance of pulsating heat pipe using nanofluid. Journal of Environmental Nanotechnology, 14(3), pp.179–188.

**Savalia, D.; P. Anadani and S. Das Lala.** (2026). Effect of surfactant on nanofluids. Discover Mechanical Engineering, 5, p.33.

**Tare, K.; U. Mukherjee and R.J. Vaidya.** (2017). Design optimization of automotive radiator cooling module. SAE Technical Paper, 2017-26-0183.

**Wang, S.; G. Xie and B. Sundén.** (2018). Numerical study of pitch effect on helical tubes. International Journal of Heat and Mass Transfer, 127, pp.1139–1153.

**Webb, R.L.** (2018). Compact heat exchangers. Journal of Enhanced Heat Transfer, 25(1), pp.1–59.